Powder Technology 330 (2018) 137–146

Contents lists available at ScienceDirect

Powder Technology

journal homepage: www.elsevier.com/locate/powtec

An experimental investigation on stable arch formation in cohesionless granular materials using developed trapdoor test

Ali Ahmadi, Ehsan Seyedi Hosseininia *

Civil Engineering Department, Faculty of Engineering, Ferdowsi University of Mashhad, Mashhad, Iran

ARTICLE INFO

Article history:
Received 1 March 2017
Received in revised form 25 December 2017
Accepted 9 February 2018
Available online 17 February 2018

Keywords:
Arching
Granular materials
Stable arch
Trapdoor test
Gravity
Arch characteristics

ABSTRACT

Arching in granular materials is a general phenomenon that exists in different domains of engineering such as design of silos and hoppers as well as geotechnical engineering problems. Due to the interaction among particles that are flowing through an opening, an arch-like structure comes into existence that causes the particles to be in a stationary state. Few researches have explored the formation of stable arches. In this study, the characteristics of statically stable arches generated in purely cohesionless granular materials are investigated experimentally. A developed form of the so-called trapdoor test was implemented in which, the opening width can be increased incrementally. The test box can also be inclined with respect to the horizontal direction in order to consider the gravity effect on the arch formation. Investigations on the self-supported arches indicate that the arch height increases as the arch width increases. However, there is fall in the height of the critical arch, which is the arch with the biggest possible width. The results also indicate that the frictional parameters of granular materials have major influence on the arch formation. The dimensions of stable arches are a function of the peak friction angle, while the critical state friction angle dominates the height of the critical arch. Furthermore, the results show that the unit weight of the granular materials has minor effect on the critical arch formation rather than frictional parameters.

1. Introduction

Arching is a general phenomenon in granular materials that is generated from interactions among contacting particles. Due to particulate nature of the soil, arching effect has been widely studied in different domains of geotechnical engineering problems such as underground structures [1,2], soil reinforcement with pile [3–5] and geosynthetic layers [6,7], and earth pressure over walls [8,9]. Arching may also refer to spontaneous formation of an unsupported stable arch upon an opening during gravitational flow. Many researches have been carried out on the study of arching in hoppers [10–12] and silos [13–17].

Trapdoor test is one experimental approach to evaluate the arching effect in granular materials. Terzaghi [18] initially conducted trapdoor experiments and described the arching effect as the load transfer through granular materials. Many other researchers performed this test with various goals [19–23].

The formation of stable arches in granular materials is an interesting issue in different domains of engineering. The challenge in this regard is that for purely cohesionless granular materials, the conventional continuum mechanics predicts no formation of stable arches [12,24,25], which is inconsistent with experimental observations. Therefore, more experimental investigation on the arch formation in such stress-free surface problems is priority.

In the literature, there is limited number of studies focused on the formation of stable arches. Sakaguchi et al. [26] tried to interpret the mechanism of arch formation and plugging of granular flow of spherical particles by using a structural method. Hidalgo et al. [27] derived an expression for the shape of arch between two rough vertical walls. They both found that the arch had a parabolic shape if it was isolated from around medium. McCue and Hill [12] derived a solution for free-surface problems within the framework of continuum mechanics and showed that, in contrast with experiments, no arch could form in cohesionless materials. Pardo and Sáez [25] performed trapdoor tests using coarse sand and then examined the ability of two different elastic-plastic constitutive soil models including Mohr Coulomb model and a multi-surface yielding model (called as Hujeux) to reproduce this phenomenon. They concluded that both constitutive models satisfactorily reproduced the soil displacement field with some small errors; however, larger differences between both models were found regarding the redistribution of stresses. In case of using the simple Mohr-Coulomb model, the best result pertains to the condition where a traction cutoff (in terms of cohesion) is considered in order to simulate the arching effect. Guo and Zhou [28] presented experimental and analytical investigations on the formation of stable arches via granular materials. In their research, they presented an apparatus in which, a single layer of nearly mono-sized particles were

* Corresponding author.
E-mail address: eseyedi@um.ac.ir (E. Seyedi Hosseininia).

https://doi.org/10.1016/j.powtec.2018.02.011
0032-5910/

placed on an inclined base plate in order to simulate plain strain condition. They focused on the critical width of stable arches formed in spherical beads and coarse sand by using a modified trapdoor test. Based on the experimental results, they showed that the critical arch width after which, no stable arch is formed, is approximately five to seven times particle size. They also concluded that the friction angle has a minor effect on the critical width rather than the cohesion. Furthermore, by using a micromechanical analysis approach, they showed that stable arches may form in cohesionless granular materials. When yielding takes place in the material, however, such condition can only be satisfied in granular materials with cohesion.

In the literature, there is a debate about the existence of such a critical outlet size above which clogging is not possible [29–33]. Chevalier et al. [19] performed some experimental and numerical (by using discrete element method) trapdoor tests and showed that the load transfer in the arch is a function of macro-mechanical frictional parameters of the soil. No effort was done in any research on the study of the characteristics of stable arches before the last stable arch collapses.

In the present study, a new developed trapdoor apparatus is implemented in order to investigate more accurately the formation of stable arches in cohesionless granular materials. The apparatus is comparable with the one presented by Guo and Zhou [28] from two viewpoints. Firstly, the inclination angle of the base plate can be changed in order to study the gravity effect. Secondly, the trapdoor width is variable in small increments and thus, it facilitates to trace the changes of dimensions of self-supporting stable arches before the arch collapses.

2. Description of developed trapdoor apparatus

Fig. 1 shows different parts of the developed trapdoor apparatus in detail. It consists of main base, two arms and supporting base. According to Fig. 1a, the main base, which holds the test box, can be inclined in different inclinations from zero to 90° with respect to the horizontal (θ). The main box is made up of a wooden board with the dimensions of 550 × 400 × 15 mm on which, a plexiglass sheet, lateral shoulders, horizontal rails and bottom box are installed (Fig. 1b). Lateral shoulders are two vertical wooden segments with 415 × 50 × 35 mm dimensions. Plexiglass is located through a groove on the inner side of the shoulders. Two horizontal movable rails are placed at the bottom to generate an opening as for trapdoor whose width is extendable to 300 mm. The space delimited to the main base, plexiglass, lateral shoulders and horizontal rails is considered as test box with the area of 300 × 400 mm. The thickness of the test box is adjustable in order to only place a single layer of materials to simulate plane strain condition as explained by Guo and Zhou [28]. A gap of 1 to 2 mm is considered between the plexiglass and the particles which causes particles to slide downward easily without confinement in perpendicular direction and thus, the influence of side friction on flowing particles gets minimized (nearly zero).

3. Experimental tests

3.1. Test materials

Spherical plastic beads and gravel packing were chosen as cohesionless ideal and angular granular materials, respectively. Fig. 2 illustrates the snapshots of these materials. The plastic beads are a set of mono-sized grains with 12 mm diameter. Gravel packing is a set of nearly-uniform coarse aggregate with coefficient of uniformity ($C_u = d_{60}/d_{10}$) of 1.3 with mean grain diameter (d_{50}) of 8.8 mm. d_x is the grain diameter in such a way that x percent (in volume) of the grains are smaller than d_x. Gravel packing was dried in oven before performing the tests.

In order to compare the particle shape of the materials in this study, the characteristics of the particles shape are presented here in terms of roundness (R), sphericity (S), and regularity (ρ) according to the visual classification method proposed by Powers [34] and modified later by Krumbein and Sloss [35]. Roundness (cf. angularity) describes the scale of major surface features while sphericity (cf. eccentricity or platiness) refers to the global form of the particle and reflects the similarity between the particle's length, height, and width [36]. Regularity is the average of roundness and sphericity, i.e., $\rho = (S + R)/2$. Based on the definitions and visual inspection, the shape of the plastic beads is considered as well-rounded with $S = 1$, $R = 1$, and $\rho = 1$ and for the gravel packing, the particles are classified as sub-rounded with S ~0.70, R ~0.49, and ρ ~0.60.

For spherical plastic beads, two different layouts of particles were considered in order to simulate loose and dense states as shown in Fig. 3. The difference in the grains arrangement leads to have samples with different peak frictional angles due to the interlocking effect among the grains [37]. As the first array related to loose state, the grains are laid down, according to Fig. 3a, in a column-like manner with a void ratio of e = 0.27. The second array corresponding to dense state, as shown in Fig. 3b, is achieved in a way that the center of each bead in even rows is situated between two lower beads in the odd rows and thus, the minimum void ratio is achieved (e = 0.10). For gravel packing, only one density was considered because only one layer of the granular materials exists in the test box and it was hardly possible to have the

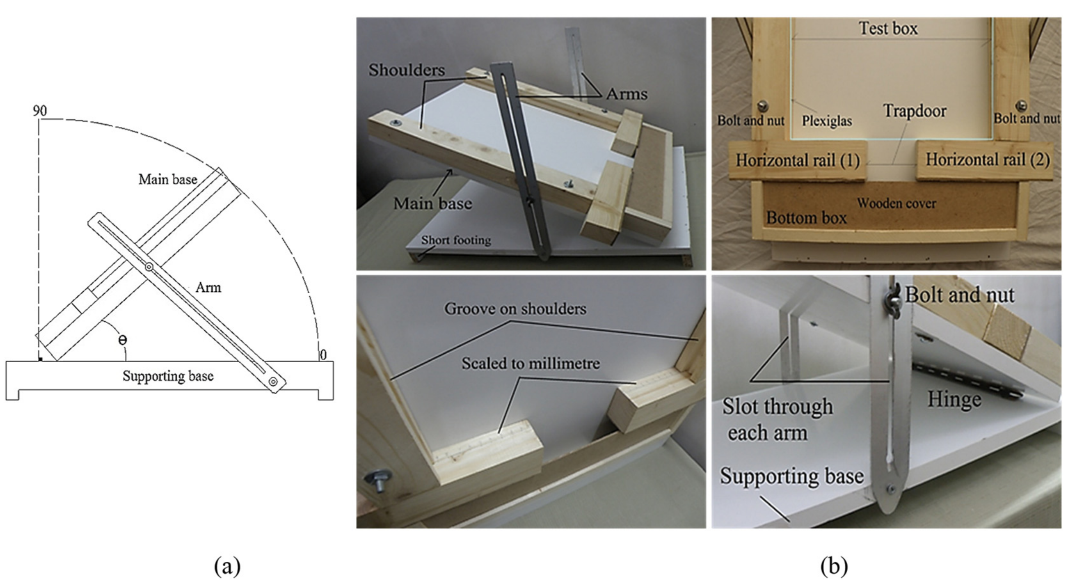

Fig. 1. View of the developed trapdoor test apparatus: (a) side view; (b) detailed view.

Fig. 2. Schematics of granular materials used in the tests: (a) plastic beads; (b) gravel packing.

tests with the same packing density in all inclination angles (θ), whose value was dominant for the highest gravity level ($\theta = 90°$). The density of the samples was determined by having the weight of the materials divided by the volume of test box.

The size of the grains was so big that the friction angle cannot be obtained from conventional geotechnical tests (e.g., triaxial and direct shear tests). Alternatively, the angle of repose was measured according to ASTM Standard C1444 [38], which can be regarded as critical state friction angle (ϕ_{cv}). Tilt box test was used to estimate the peak friction angle (ϕ_{peak}) of the materials, which results in the determination of mobilized friction angle at a very low effective normal stress [39,40]. The values of density as well as different friction angles are presented in Table 1 for three cases of materials. The obtained values of ϕ_{cv} and ϕ_{peak} are in good agreement with other experiments [41–43].

3.2. Test procedure

In this research, the trapdoor tests for each granular material (beads in loose and dense states as well as gravel packing) were performed for every 10-degree increments of the inclination angle (θ) from 10 to 90°. Performing the tests with different inclination angles is useful to study the trend of arch formation as well as arch sizes by increasing the gravity. For a specific θ, each test includes a series of runs in which, the width of the trapdoor was increased 2 mm. The process of each run includes the following steps: (1) after fixing the test box at desired inclination angle (θ), the horizontal rails in a symmetrical manner are tuned such that the desired opening is blocked by a trapdoor. The test box is then filled with granular materials; (2) the trapdoor moves downward slowly and let the grains to be discharged out; (3) a statically stable arch-shaped structure may be formed over the trapdoor which stops the process of exiting grains. The dimensions of the stable arch are measured; (4) the next run of the test is repeated from the beginning with an increased trapdoor width (plus 2 mm) until no stable arch appears on the horizontal rails and flow happens for remain of the grains. Each test series was repeated at least twice in order to minimize the effect of probable errors in the experiments.

4. Observations and discussion

Fig. 4 indicates the stable arches generated over the rails in different granular materials for $\theta = 90°$. Since the grains are purely cohesionless, the sole factor influencing the arch formation is the interlocking effect among the grains.

4.1. Stable arch formation

To follow how a stable arch can be generated, a number of photos in series with the intervals of 0.2 s were taken from the test box from the start of trapdoor removal to the moment of arch formation. As an example, the results for the gravel packing with the fixed trapdoor width of 40 mm and the inclination angle of $\theta = 90$ is presented in Fig. 5. After removing the trapdoor, a mass of grains move towards the opening to

Fig. 3. Arrays of the plastic beads: (a) loose state; (b) dense state.

Table 1
Characteristic of granular materials used in the tests.

Parameter			Beads (loose state)	Beads (dense state)	Gravel packing
Mean grain size	d_{50}	[mm]	12	12	9
Density	ρ	[gr/cm^3]	0.96	1.05	1.58
Critical state friction angle (angle of repose)	ϕ_{cv}	[degree]	23	23	30
Peak friction angle	ϕ_{peak}	[degree]	23	37	45

be discharged. As shown in Fig. 5 (parts a to f), three regions can be distinguished in all the moments before a stable arch is formed over the opening. These regions are separated visually by boundaries which are highlighted in the figures. The first region is located above the opening in which, the grains tend to be discharged with high speed and a funnel-like region is formed and flow occurs. At the onset of soil failure, the boundaries of this region are vertical, but they become inclined in such a way that the upper part widens. However, the flow region becomes narrower by reaching the time of arch formation. The second region corresponds to the grains situated in the sides of the opening that are discharged less slowly. This region can be detected by comparing several continuous snapshots with together. This region is separated from the third region where the grains are stagnant without any movement. The boundary between the last two regions is a line with a nearly-fixed angle of $\theta_0 = 58$ to 62 from the horizontal. The observed mechanism explained above is very close to that described by Terzaghi [44], who defined vertical and inclined slip lines in a yielding soil caused by a downward moving trapdoor. He then used this failure mechanism in analytical solutions for the estimation of applied load over the tunnel lining caused by arching effect. According to his analysis, which is based on Mohr-Coulomb failure criterion, the stagnant section of the soil is separated by a line with an angle of $\theta_0 = 45 + \phi/2$ (where ϕ is a type of soil internal friction angle), which is consistent with the observations in this research if $\phi = \phi_{cv}$ (=30) is adopted. The same observation was reported by Guo and Zhou [28]. Referring back to Figs. 5d and e, the grains over the side rails and close to the opening tend to be stationary and the wall of a stable arch is built progressively. This phenomenon can be explained by the mobilization of shear strength of granular materials which is defined by the rolling and interlocking resistance of particles. The stationary region of the soil is gradually enlarged and flow region becomes narrower until the body of a stable arch is formed as depicted in Fig. 5f. According to the observations experienced in this research, the wall construction of the arch takes long time (about 1.4–1.8 s), but the arch closure at the upper parts happens rapidly (About 0.4 s).

In order to more precisely inspect the formation of statically stable arches over different trapdoor widths, the geometry and the dimension labels of an arch are defined according to Fig. 6. A crown and two abutments are considered for the geometry of each stable arch according to Fig. 6a. A Cartesian coordinate system (x-y) is defined with an origin at the location of the upper edge of the rails and the middle point between them. According to Fig. 6b, the width of the opening is the trapdoor width (W) and the internal distance between two abutments is defined as the arch width (B). The vertical distance from the origin to the lower side of the crown is defined as the arch height (H). Since two different mean grain size (d_{50}) were used in the tests, the normalized values H/d_{50}, W/d_{50} and B/d_{50} are considered in the presentations of the results.

In all the test series, arch width (B) was measured in addition to the width of the trapdoor (W). The variation of normalized arch width (B/d_{50}) versus the normalized trapdoor width (W/d_{50}) of all the test series is presented in Fig. 7 for $\theta = 10, 40, 70$, and 90°, separately. It can be found out that, the arch width (B) is not always equal to the trapdoor width (W) and we have: $B = (0.75\,to\,1.15)W$. This means that for the range of the tested materials in this study, the abutments of the arches are not necessarily generated at the edge of the trapdoor, but they may be formed with an offset from the edges. It can be expected that the value of the arch width (B) would become closer to that of the trapdoor width (W) as the grain size becomes finer.

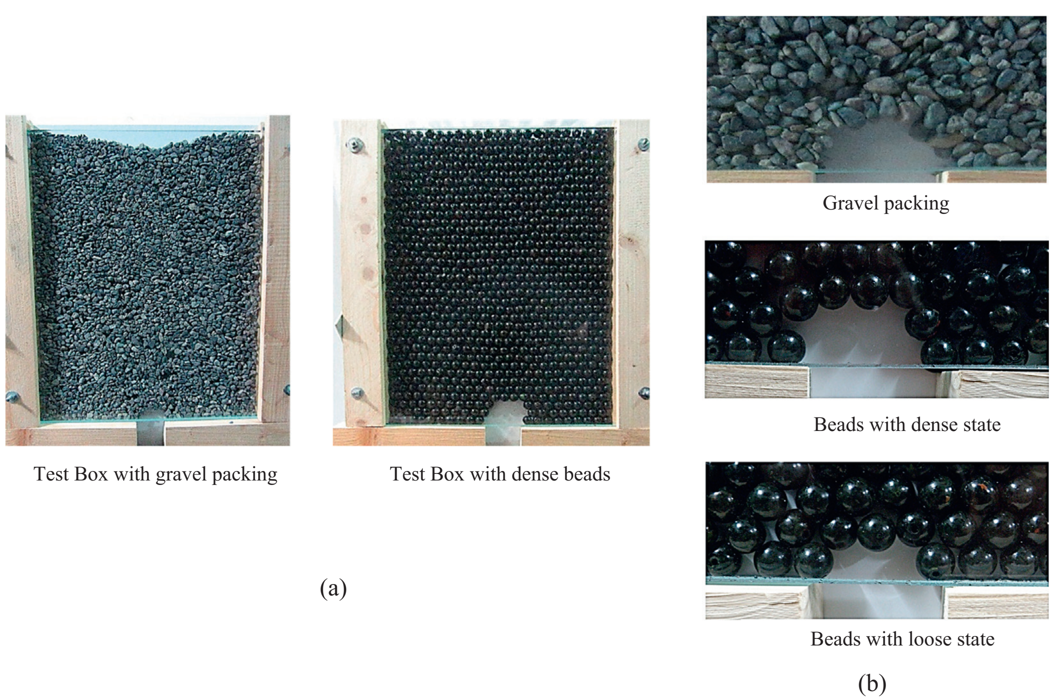

Fig. 4. Formation of stable arches over the trapdoor in different granular materials for $\theta = 90°$: (a) General view of the test box; (b) Close view of three sets of materials.

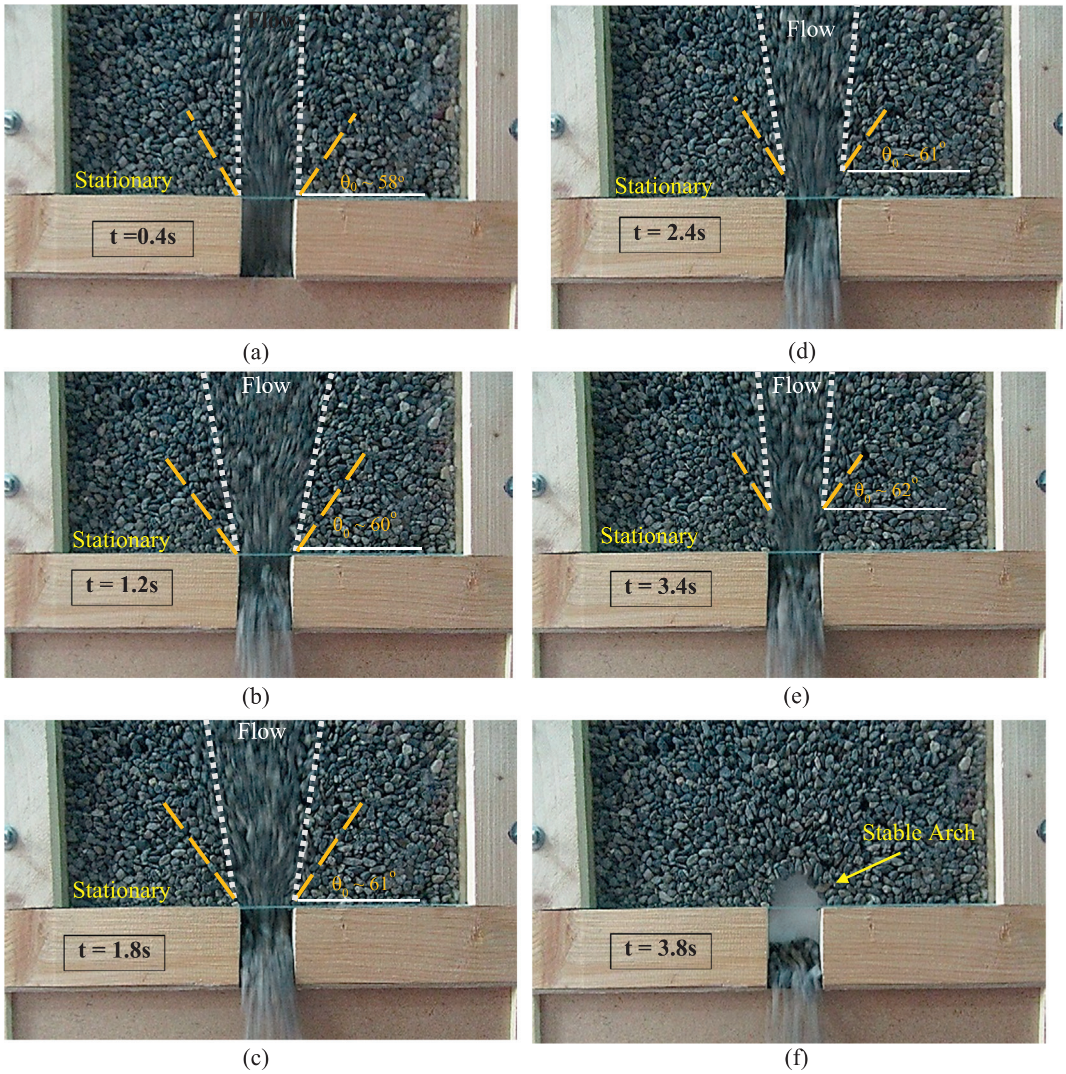

Fig. 5. Presentation of the flow and the generation of stable arch during the time for gravel packing after the trapdoor test is removed. Fine dash line represents the flow part and the coarse dash line shows the boundary between moving and stationary grains. ($t = 0$ corresponds to the trapdoor removal time).

The variation of the normalized arch height (H/d_{50}) with the normalized arch width (B/d_{50}) is depicted in Fig. 8 for $\theta = 10$, 40, 70, and 90°. For small arches (corresponding to $B/d_{50} < 2.5$ to 3.0), the arch height in three samples are the same. However, for bigger arch widths, the trend in the curves is deviated from each other. As for the other observation in the graphs, it can be found out that the critical height, which refers to the height of the last possible sable arch, is always smaller than that at one stage before it. In other words, the arch behaves as a ductile material and the onset of arch collapse can be recognized by a fall in height.

The formation and collapse of stable arches can be studied by focusing on the shear strength of granular materials. From the micromechanical viewpoint, the generation of force chain among particles is the main reason to cause the construction of arch structures in the mass of granular materials. In the absence of cohesion, the stability of such structures is solely influenced by the mobilized shear strength among particles. It is

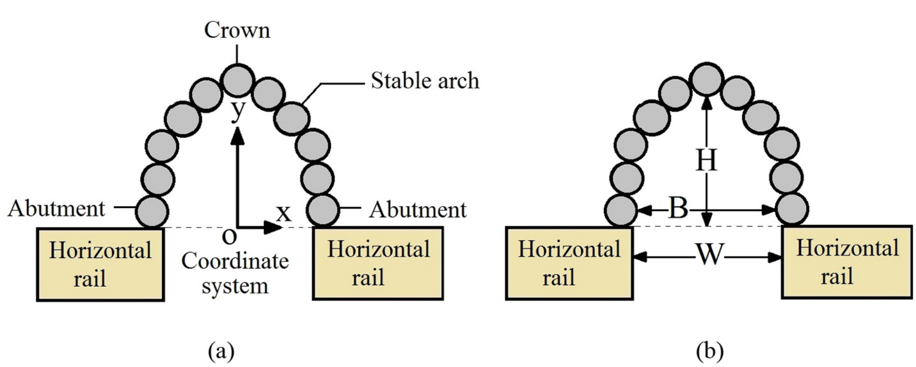

Fig. 6. Definition of the geometry of the arches: (a) parts and coordinate system; (b) arch width and height and trapdoor width.

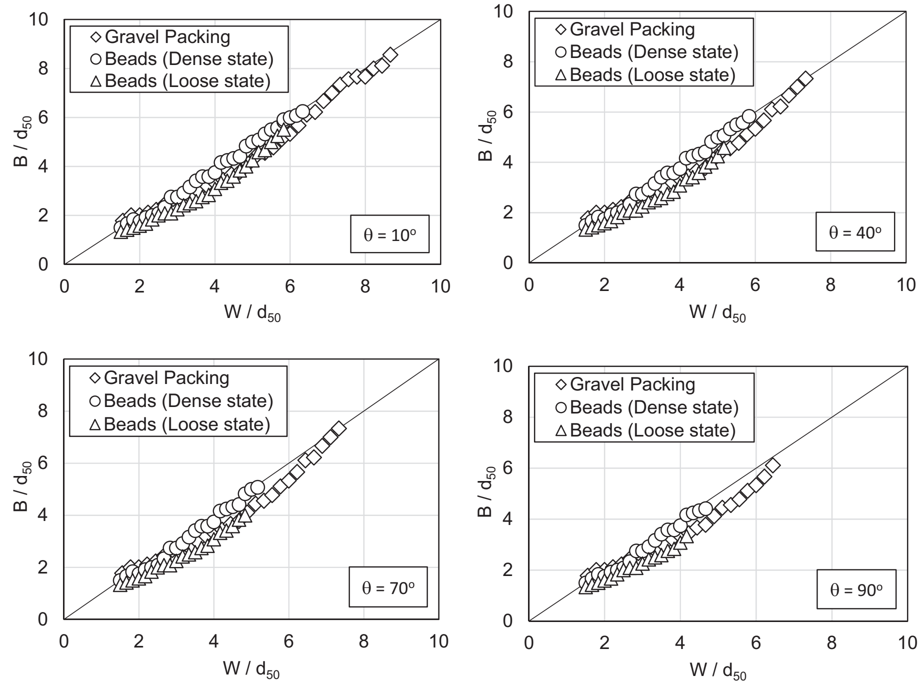

Fig. 7. Variation of normalized arch width versus the normalized trapdoor width for different inclination angles.

already known that for purely cohesionless granular materials, the shear strength (τ_f) obeys the frictional Coulomb law by the simple formula: $\tau_f = \sigma_n \tan \varphi_{mob}$, where σ_n is normal stress and ϕ_{mob} is the mobilized friction angle. The maximum shear strength corresponds to the peak friction angle (ϕ_{peak}), which occurs at small deformation, while the friction angle at the critical state (ϕ_{cv}) governs the shear strength when large deformation occurs in the material. If the applied force on the particle-formed structure causes that the shear stress exceeds the shear strength of the mass (corresponding to the critical state), the structure collapses. The effect of shear strength on the arch formation is discussed in the following.

4.2. Effect of mobilized friction angle

The variation of normalized arch height (H/d_{50}) with the normalized trapdoor width (W/d_{50}) for the tested granular materials is depicted in Fig. 9 in four groups of $\theta = 10$, 40, 70, and 90°. Excluding the fall in the height, which is related to the critical arch, it is interesting to see that although the loose and dense beads have the same physical property, the results of the gravel packing and dense beads coincide and the growth rate is bigger than that of the loose beads. It is reminded that in the statically-stable arches, the maximal load transfer governs among the particles and thus, the mobilized friction angle can be regarded as to be

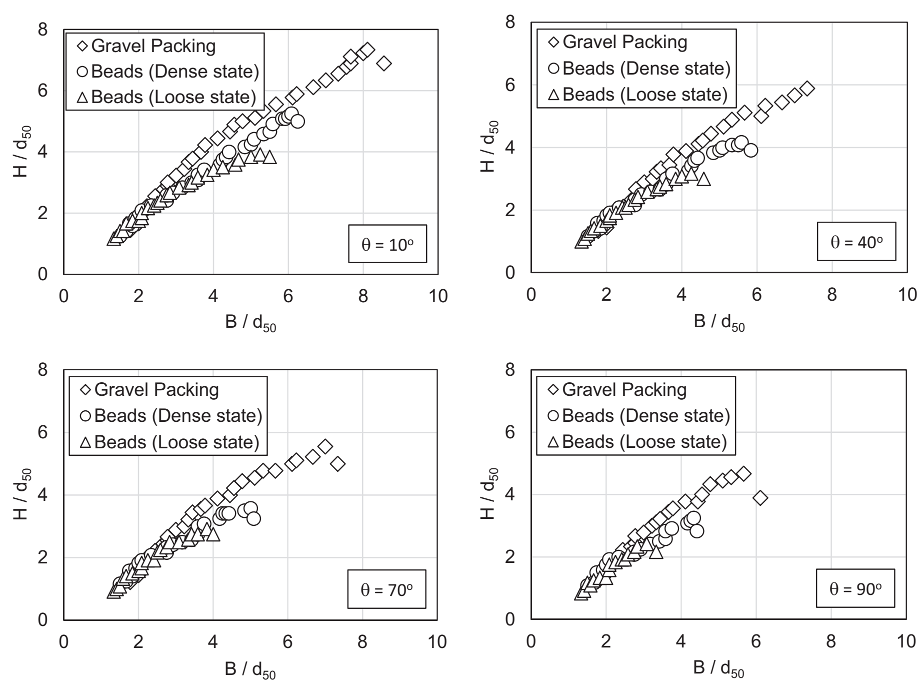

Fig. 8. Variation of normalized arch height versus the normalized arch width for different inclination angles.

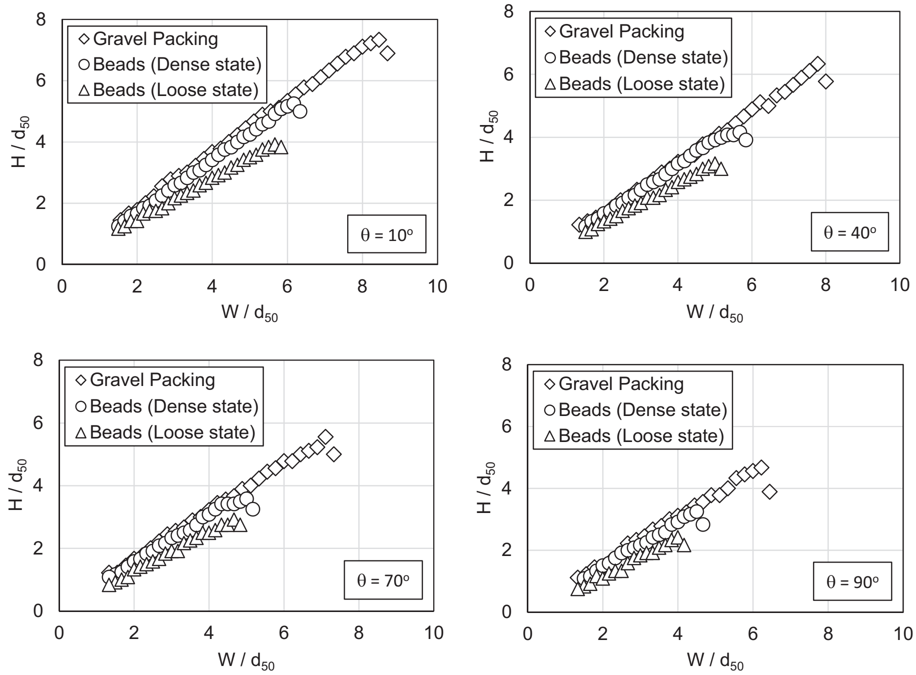

Fig. 9. Variation of normalized arch height versus the normalized trapdoor width for different inclination angles.

the peak friction angle. Hence, the coincidence of dense beads and gravel packing curves is justifiable according to the peak friction angles ($\phi_{peak} = 37, 45°$ for dense beads and gravel packing respectively in comparison with $\phi_{peak} = 23°$ for loose beads). This phenomenon was described by Chevalier et al. [19], who studied experimentally and numerically the influence of macro-mechanical frictional parameters on trapdoor problems. They performed several trapdoor tests in the laboratory with a downward moving door and the imposed pressure from the soil over the trapdoor (i.e., load transfer response) was measured. They found that at the initial movement of the trapdoor, which corresponds to the initiation of arching effect, the applied pressure over the trapdoor is minimal and the value can be verified well with analytical solution of

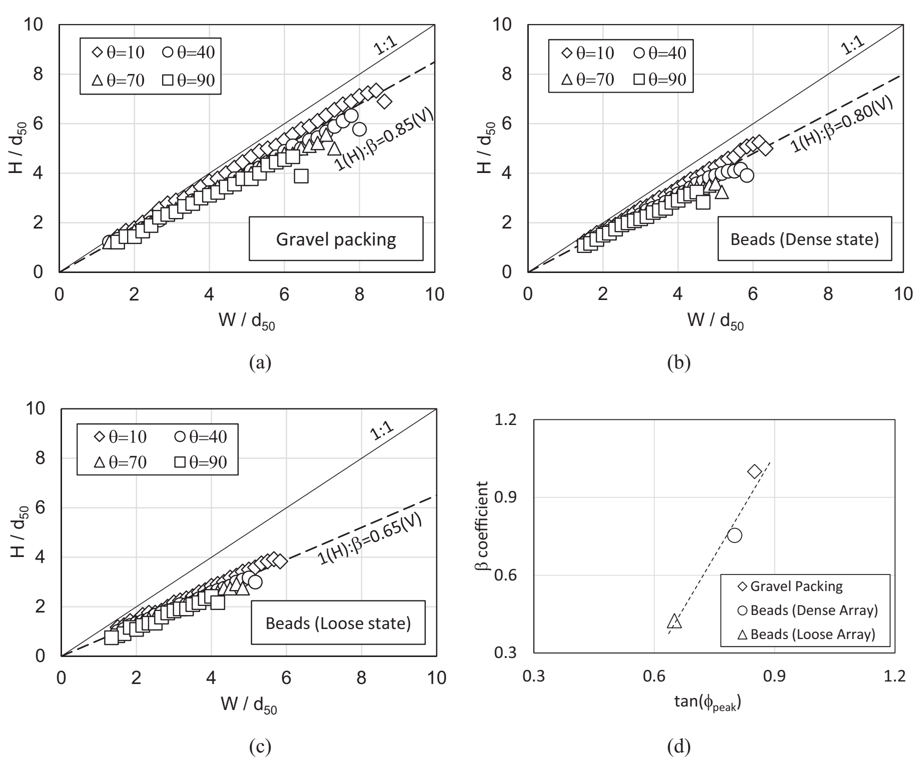

Fig. 10. Effect of peak friction angle on the generation of stable arches: variation of normalized arch height versus the normalized trapdoor width for (a) gravel packing; (b) dense beads; (c) loose beads; (d) variation of β with tangent of peak friction angle.

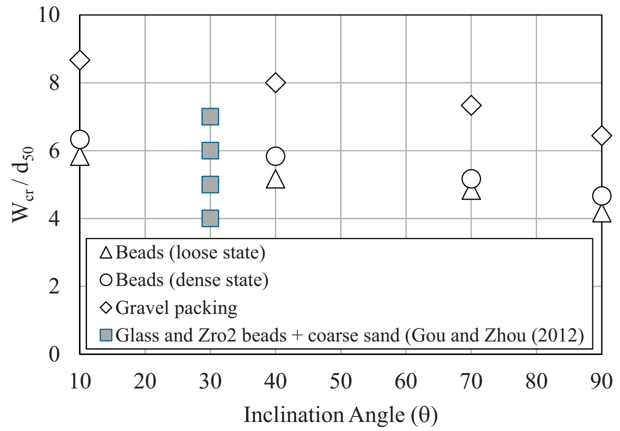

Fig. 11. Variation of normalized critical trapdoor width with different inclination angles.

Terzaghi [18] if peak friction angle (ϕ_{peak}) is used. They also experienced the same results with numerical simulations using discrete element method.

If the H/d_{50} vs. W/d_{50} curves of each granular material are drawn separately with different inclination angles (θ), as shown in Fig. 10 (parts a, b, and c), the results are almost coincident for any value of θ. This means that the gravity has no effect on the stable arch formation. This finding seems to match well the results of centrifuge tests performed by Mathews and Wu [45], who investigated silo discharge and internal silo flow patterns. They reported that observed flow patterns are independent of gravity. Excluding the critical arch (the last point after which the arch collapses), a line with slope of β can be defined between H and W:

$$H = \beta . W \tag{1}$$

where β can be estimated as 0.65 for loose array of beads, 0.85 for dense array of beads, and 0.85 for gravel packing. According to Fig. 10d, there is a straight-forward relationship between β and tan(ϕ_{peak}). By this graph and based on these experiments, it is not intended to say that there is a linear relationship between them; however, it can be deduced that the relationship between the arch height and trapdoor width can be defined as to be dependent to peak friction angle. This finding is also in good agreement with the results presented by Guo and Zhou [28], who found that $H = W \cdot \tan(\alpha/4)$, where α is the angle of the wall arch with respect to the horizontal. They declared that α increases as the packing density (and hence peak friction angle) increases.

In all the tests, the last possible stable arch, i.e., critical arch, was generated when the granular material was at the onset of large movement in which, the mobilized friction angle corresponds to the critical state. Chevalier et al. [19] demonstrated that by increasing the trapdoor movement, the arching effect comes to be disappeared and the value of load transfer response matches well with the analytical solution if the critical state friction angle is used. Fig. 11 shows the value of critical arch height ratio (H_{cr}/d_{50}) with different θ. It can be seen that totally, the results of loose and dense beads are close to each other since they have the same critical state friction angle (ϕ_{cv}=23°). However, H_{cr}/d_{50} of the gravel packing is much higher. The results in this research agree well with the range of values obtained by Guo and Zhou [28].

In order to understand the effect of unit weight of granular materials on the critical arch formation, the variation of normalized parameters H_{cr}/d_{50} and W_{cr}/d_{50} with equivalent unit weight (=ρgsinθ) are sketched in Fig. 12. As seen, the normalized critical arch height as well as the critical trapdoor width decreases as the equivalent unit weight increases. Although the results of the loose and dense beads coincide, the results of the gravel packing are separated, but both follow a decreasing trend with almost the same rate. This means that the unit weight of the materials has much less effect on the characteristics of the critical height in comparison with the frictional parameters. This finding is in good agreement with numerical as well as experimental tests. Numerical simulations performed by Zuriguel et al. [46] and Arévalo and Zuriguel [47] about the effect of driving force on the clogging of granular materials showed that the gravity does not have crucial role on the development of the aperture size. Dorbolo et al. [41] experimentally examined the effect of gravity on the discharge of granular materials in silos by using centrifuge physical models. They found that the critical aperture size below which the flow is jammed, does not significantly increase with the apparent gravity.

4.3. Geometrical shape of the stable arches

By investigating the geometry of the generated arches over the trapdoor, it can be said that the arches generally have a symmetric shape similar to a parabola. Considering the Cartesian x-y coordinate system according to Fig. 5, a second-order form of parabola equation is suggested for the outline of a stable arch:

$$\frac{y}{H} = \left(1 - \frac{2x}{B}\right)^2 \tag{2}$$

Considering Eq. (1) and assuming that $B \approx W$, the following expression can be obtained as a function of trapdoor width:

$$y = \beta\left(1 - \frac{2x}{W}\right)^2 W \tag{3}$$

where β depends on the packing density and the value is the same as obtained from Eq. (1). The measured outlines of stable arches for different trapdoor widths (W = 20, 36, 54 mm) are sketched in the x-y plane and the results are presented in Fig. 13. In the same Figure, the predicted outline of the arches using Eq. (3) is depicted. It can be seen that the predictions are acceptable for a wide range of inclination angles and trapdoor widths.

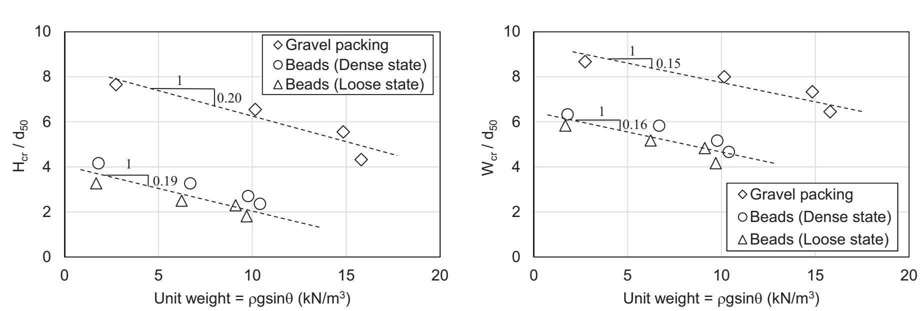

Fig. 12. Variation of normalized critical arch height and critical trapdoor width versus equivalent unit weight of the materials.

5. Conclusion

In this paper, the generation of self-supported arches over different trapdoor widths was investigated experimentally. A new developed trapdoor test was designed and implemented in which, the trapdoor width can be increased incrementally and the characteristics of stable arches as well as the critical ach was studied. Furthermore, the effect of the gravity on the results was investigated by different inclination

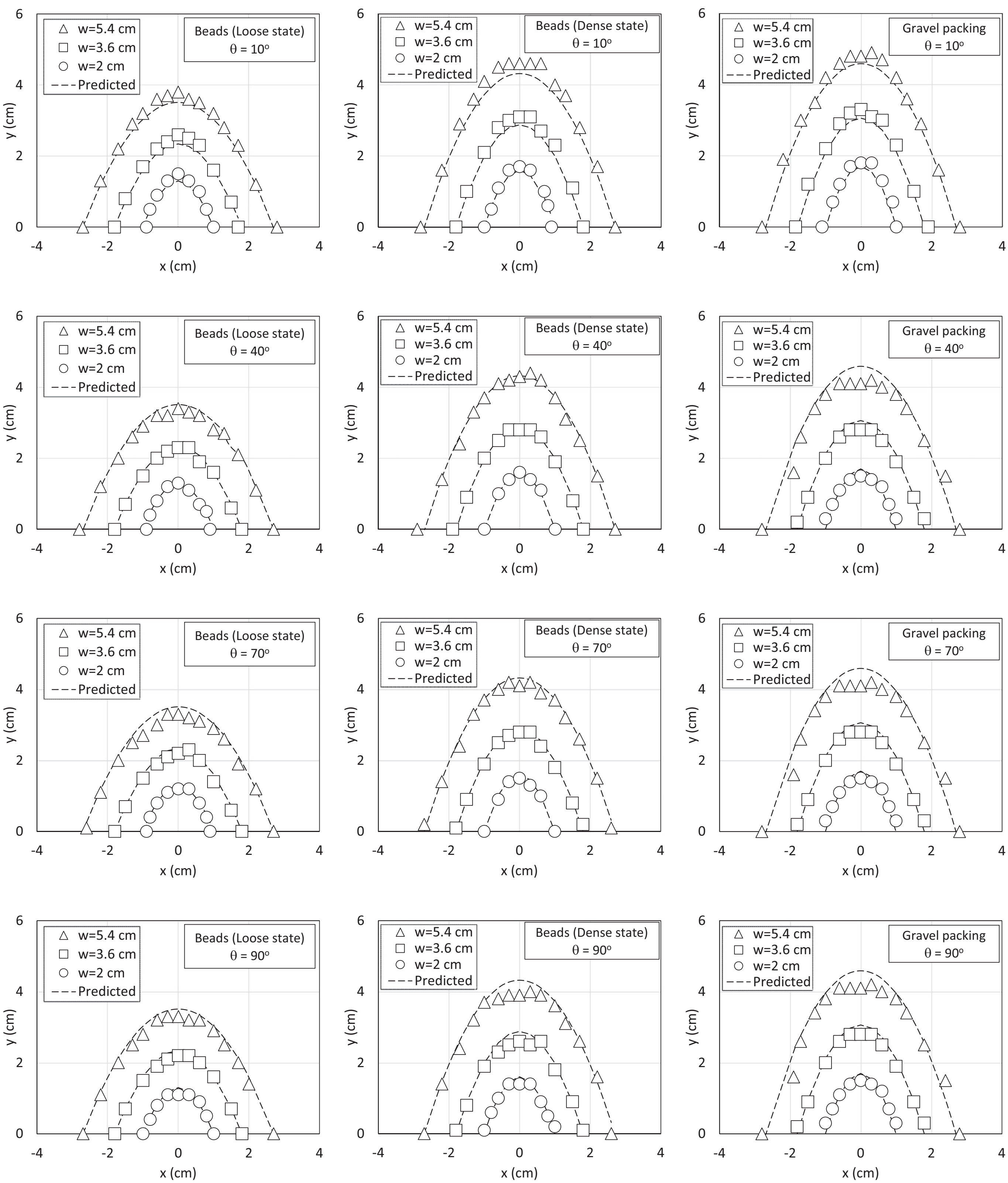

Fig. 13. Presentation of stable arch geometry in the x-y coordinate system: measurement versus the predictions from Eq. (3) for different inclinations angles.

angles of the text box. The main conclusions may be drawn from this study as follows:

- Over an opening, statically stable arches can be generated with the ratio of trapdoor width to mean grain size in the range of $W/d_{50} = 2$ to 8.
- For the tested materials, the arch width is not necessarily equal to the trapdoor width and a stable arch may be generated with bigger width over the trapdoor.
- The peak friction angle is the main parameter to control the stability and dimension of the statically-stable arches.
- The height of the last possible arch, which is called here as critical height, is not the highest arch, but the arch crown shows a decrease in height before it collapses.
- There is direct relationship between the width and height of stable arches which is a function of the density of the granular material.
- The onset of arch instability i.e., arch collapse, is related to the shear strength of the granular material when the soil is to experience large deformation whose friction angle is defined as the critical state friction angle.
- The unit weight of granular materials does not have significant effect on the arch instability. Rather, the frictional parameters especially the critical state friction angle, influences greatly on the critical arch formation with respect to the unit weight.

It is noted that the results of this paper is limited to the characteristics of the materials used in the tests. Some other factors such as particle shape, particle gradation and possible inter-particle cohesion would influence the results which are proposed for future researches.

References

[1] C.N. Chen, W.-Y. Huang, C.-T. Tseng, Stress redistribution and ground arch development during tunneling, Tunn. Undergr. Space Technol. 26 (2011) 228–235.
[2] C.J. Lee, B.R. Wu, H.T. Chen, K.H. Chiang, Tunnel stability and arching effects during tunneling in soft clayey soil, Tunn. Undergr. Space Technol. 21 (2006) 119–132.
[3] S.W. Abusharar, J.J. Zheng, B.G. Chen, J.H. Yin, A simplified method for analysis of a piled embankment reinforced with geosynthetics, Geotext. Geomembr. 27 (2009) 39–52.
[4] A. Shelke, S. Mishra, Uplift capacity of single bent pile and pile group considering arching effects in sand, Geotech. Geol. Eng. 2010 (2010) 337–347.
[5] X. Li, X. Pei, M. Gutierrez, S. He, Optimal location of piles in slope stabilization by limit analysis, Acta Geotech. 7 (2012) 253–259.
[6] B. Le Hello, P. Villard, Embankments reinforced by piles and geosynthetics—numerical and experimental studies dealing with the transfer of load on the soil embankment, Eng. Geol. 106 (2009) 78–91.
[7] B. Zhu, D. Gao, J.-c. Li, Y.-m. Chen, Model tests on interaction between soil and geosynthetics subjected to localized subsidence in landfills, J. Zhejiang Univ. Sci. A 13 (2012) 433–444.
[8] G. Qiu, J. Grabe, Active earth pressure shielding in quay wall constructions: numerical modeling, Acta Geotech. 7 (2012) 343–355.
[9] K.H. Paik, R. Salgado, Estimation of active earth pressure against rigid retaining walls considering arching effects, Géotechnique 53 (2003) 643–653.
[10] A. Drescher, A.J. Waters, C.A. Rhoades, Arching in hoppers: I. Arching theories and bulk material flow properties, Powder Technol. 84 (1995) 165–176.
[11] S. Jing, H. Li, An experimental study on the mechanics of arching in hoppers connected to a moving bed with negative pressure gradient, Powder Technol. 95 (1998) 143–151.
[12] S.W. McCue, J.M. Hill, Free surface problems for static Coulomb-Mohr granular solids, Math. Mech. Sol. 10 (2005) 651–672.
[13] Miccio, Barletta, Poletto, Flow properties and arching behavior of biomass particulate solids, Powder Technol. 235 (2013) 312–321.
[14] I. Oldal, I. Keppler, B. Csizmadia, L. Fenyvesi, Outflow properties of silos: the effect of arching, Adv. Powder Technol. 23 (2012) 290–297.
[15] A. Cannavacciuolo, D. Barletta, G. Donsì, G. Ferrari, M. Poletto, Arch-free flow in aerated silo discharge of cohesive powders, Powder Technol. 191 (2009) 272–279.
[16] A. Garcimartín, I. Zuriguel, L.A. Pugnaloni, A. Janda, Shape of jamming arches in two-dimensional deposits of granular materials, Phys. Rev. E 82 (2010), 031306.
[17] K. To, P.-Y. Lai, Jamming pattern in a two-dimensional hopper, Phys. Rev. E 66 (2002), 011308.
[18] K. Terzaghi, Stress Distribution in Dry and in Saturated Sand Above a Yielding Trap-Door, First International Conference on Soil Mechanics and Foundation Engineering Cambridge, Massachusetts, 1936 307–311.
[19] B. Chevalier, G. Combe, P. Villard, Experimental and discrete element modeling studies of the trapdoor problem: influence of the macro-mechanical frictional parameters, Acta Geotech. 7 (2012) 15–39.
[20] C.H. Evans, An examination of arching in granular soils, Dept. of Civil Engineering, Massachusetts Institute of Technology, 1984.
[21] B. Ladanyi, B. Hoyaux, A study of the trap-door problem in a granular mass, Can. Geotech. J. 6 (1969) 1–14.
[22] I. Vardoulakis, B. Garf, G. Gudehus, Trap-door problem with dry sand: a statical approach based upon model test kinematics, Int. J. Numer. Anal. Methods Geomech. 5 (1981) 57–78.
[23] Y.D. Costa, J.G. Zornberg, B. Bueno, S.C.L. Costa, Failure mechanisms in sand over a deep active trapdoor, J. Geotech. Geoenviron. 135 (2009) 1741–1753.
[24] V.V. Sokolovskii, Statics of Granular Media, Pergamon, New York, 1965.
[25] G.S. Pardo, E. Sáez, Experimental and numerical study of arching soil effect in coarse sand, Comput. Geotech. 57 (2014) 75–84.
[26] H. Sakaguchi, E. Ozaki, M. Tanaka, Some relation between stability of arches and plugging of granular materials, Sci. Rep. Faculty Agric. 20 (1993) 225–229.
[27] R. Hidalgo, H. Herrmann, E. Parteli, F. Kun, Force chains in granular packings, The Physics of Complex Systems: Varenna Proceedings Course CLV, IOS Press, AMsterdam 2004, pp. 153–171.
[28] P. Guo, S. Zhou, Arch in granular materials as a free surface problem, Int. J. Numer. Anal. Methods Geomech. 37 (2012) 1048–1065.
[29] K. To, P.-Y. Lai, H.K. Pak, Jamming of granular flow in a two-dimensional hopper, Phys. Rev. Lett. 86 (2001) 71.
[30] I. Zuriguel, A. Garcimartín, D. Maza, L.A. Pugnaloni, J.M. Pastor, Jamming during the discharge of granular matter from a silo, Phys. Rev. E 71 (2005), 051303.
[31] K. To, Jamming transition in two-dimensional hoppers and silos, Phys. Rev. E 71 (2005) 060301(R).
[32] A. Janda, I. Zuriguel, A. Garcimartín, L.A. Pugnaloni, D. Maza, Jamming and critical outlet size in the discharge of a two-dimensional silo, Europhys. Lett. 84 (2008), 44002.
[33] C.C. Thomas, D.J. Durian, Fraction of clogging configurations sampled by granular hopper flow, Phys. Rev. Lett. 114 (2015), 178001.
[34] M.C. Powers, A new roundness scale for sedimentary particles, J. Sediment. Petrol. 23 (1953) 117–119.
[35] W.C. Krumbein, L.L. Sloss, Stratigraphy and Sedimentation, Freeman and Company, San Francisco, 1963.
[36] G.-C. Cho, J. Dodds, J.C. Santamarina, Particle shape effects on packing density, stiffness, and strength: natural and crushed sands, J. Geotech. Geoenviron. 131 (2006) 591–602.
[37] P.W. Rowe, The stress-dilatancy relation for static equilibrium of an assembly of particles in contact, Proc. Royal Soc. A (1962) 500–527.
[38] A. C1444-00, Standard Test Method for Measuring the Angle of Repose of Free-Flowing Mold Powders, ASTM, 2005.
[39] N. Barton, B. Kjaernsli, Shear strength of rockfill, J. Geotech. Eng. Div. ASCE 107 (1981) 873–891.
[40] N. Barton, Shear strength of rockfill, interfaces and rock joints, and their, J. Rock Mech. Geotech. Eng. 5 (2013) 249–261.
[41] K. Thoeni, S.G. Fityus, A. Giacomini, J. Vaha, Discrete modelling of a tilt box test for granular materials, in: Kimoto Uzuoka (Ed.), Computer Methods and Recent Advances in Geomechanics, Taylor and Francis Group, London, 2015.
[42] G. Cho, J. Dodds, J. Santamarina, Particle shape effects on packing density, stiffness, and strength: natural and crushed sands, J. Geotech. Geoenviron. 132 (2006) 591–602.
[43] A. AfzaliNejad, A. Lashkari, P.T. Shourijeh, Influence of particle shape on the shear strength and dilation of sand-woven geotextile interfaces, Geotext. Geomembr. (2017).
[44] K. Terzaghi, Theoretical Soil Mechanics, J. Wiley and Sons, Inc., 1943
[45] J.C. Mathews, W. Wu, Model tests of silo discharge in a geotechnical centrifuge, Powder Technol. 293 (2016) 3–14.
[46] I. Zuriguel, D. Maza, A. Garcimartín, Role of driving force on the clogging of inert particles in a bottleneck, Phys. Rev. E 89 (2014), 042205.
[47] R. Arévalo, I. Zuriguel, Clogging of granular materials in silos: effect of gravity and outlet size, Soft Matter 12 (2016) 123–130.